ARTICLE

Half-sandwich organometallic Ru and Rh complexes of (N,N) donor compounds: effect of ligand methylation on solution speciation and anticancer activity

Received 00th January 20xx,
Accepted 00th January 20xx

DOI: 10.1039/x0xx00000x

János P. Mészáros,[a,b,*] Veronika F.S. Pape,[c,d] Gergely Szakács,[c,e] Gábor Németi,[a] Márk Dénes,[f] Tamás Holczbauer,[f,g] Nóra V. May,[f] Éva A. Enyedy[a,b,*]

A series of half-sandwich polypyridyl complexes was synthesized and compared focusing on structural, cytotoxic and aqueous solution behaviour. The formula of the synthesized complexes is [M(arene)(N,N)Cl]Cl, where M: Ru or Rh, arene: *p*-cymene, toluene or $C_5Me_5^-$, (N,N): 2,2'-bipyridine (bpy), 4,4'-dimethyl-2,2'-bipyridine (dmb), 1,10-phenanthroline (phen) or 2,9-dimethyl-1,10-phenanthroline (neo). The structures of five half-sandwich complexes were determined by X-ray crystallography. It was found that introducing methyl groups next to the coordinating nitrogen atoms of the bidentate ligand causes steric congestion around the metal centre which changes the angle between ligand planes. The ligands and the Rh complexes showed significant cytotoxicity in A2780 and MES-SA cancer cell lines (IC_{50} = 0.1–56 μM) and in the cisplatin-resistant A2780cis cells. Paradoxically, phen and dmb as well as their half-sandwich Rh complexes showed increased toxicity against multidrug resistant MES-SA/Dx5 cells. In contrast, coordination to Ru caused loss of toxicity. Solution equilibrium constants showed that the studied metal complexes have high stability, and no dissociation was found for Ru and Rh complexes even at micromolar concentrations in a wide pH range. However, in case of Ru complexes a slow and irreversible decomposition, namely arene loss was also observed, which was more pronounced in light exposure in aqueous solution. In case of neo, the methyl groups next to the nitrogen atoms significantly decrease the stability of complexes. For Rh complexes, the order of the stability constants corrected with ligand basicity (log *K**): 9.78 (phen) > 9.01 (dmb) > 8.89 (bpy) > 3.93 (neo). The coordinated neo resulted in an enormous decrease in the chloride ion affinity of Ru compounds. Based on the results, a universal model was introduced for the prediction of chloride ion capability of half-sandwich Rh and Ru complexes. It combines the effects of the bidentate ligand and the M(arene) part using only two terms, performing multilinear regression procedure.

Introduction

Based on the success of cisplatin, complexes of other platinum group metal ions were developed and introduced into clinical trials. Ru(III) complexes, namely NAMI-A and BOLD-100 (formerly known as KP-1339)[1] and the Ru(II) containing TLD1433 entered clinical trials.[1] The proposed mechanism is that they are activated by reduction. Based on this idea several Ru(II) complexes have been synthesized, possessing an organometallic half-sandwich structure having a bidentate ligand and a monodentate leaving group. Early examples contained ethylenediamine and halide ion as ligands (the so-called RAED complexes),[1,2] which were followed by the Os(II), Ir(III) and Rh(III) analogues and with different bidentate ligands. Some of these half-sandwich complexes showed remarkable cytotoxic activity and several structure-activity relationship analyses were conducted to identify the key chemical parameters.[1,3] The mechanism of action of these compounds show a wide variety, as the RAED complexes are capable of DNA-binding,[4] enzyme inhibition (cathepsin B, thioredoxin reductase),[5,6] and the complexes of phenylazopyridines with $[Ru/Os(\eta^6\text{-}p\text{-cymene})(H_2O)_3]^{2+}$ show catalytic GSH oxidation.[7,8] The latter is the primary mechanism of the 'catalytic metallodrugs'.[9] The group of Sadler proved the occurrence of intracellular catalysis by half-sandwich complexes of (N,N) donor ligands, such as ethylenediamine, 2,2'-bipyridine (bpy) and 1,10-phenanthroline (phen).[10] The reaction of these organometallic complexes with the NAD^+/NADH pair was found in the presence of formate ions.

[a.] *Department of Inorganic and Analytical Chemistry, Interdisciplinary Excellence Centre, University of Szeged, Dóm tér 7, H-6720 Szeged, Hungary; E-mail: meszaros.janos@chem.u-szeged.hu; enyedy@chem.u-szeged.hu*
[b.] *MTA-SZTE Lendület Functional Metal Complexes Research Group, University of Szeged, Dóm tér 7, H-6720 Szeged, Hungary*
[c.] *Institute of Enzymology, Research Centre for Natural Sciences, Magyar Tudósok körútja 2, H-1117 Budapest, Hungary*
[d.] *Department of Physiology, Semmelweis University, Tűzoltó utca 37-47, H-1094 Budapest, Hungary*
[e.] *Institute of Cancer Research, Medical University of Vienna, Borschkegasse 8a, A-1090 Vienna, Austria*
[f.] *Centre for Structural Science, Research Centre for Natural Sciences, Magyar tudósok körútja 2, H-1117 Budapest, Hungary*
[g.] *Institute of Organic Chemistry, Research Centre for Natural Sciences, Magyar tudósok körútja 2, H-1117 Budapest, Hungary*

†Electronic Supplementary Information (ESI) available: ^1H and ^{13}C NMR spectra of complexes, list of NMR peaks, ESI-MS spectra, crystallographic data and additional spectra about aqueous stability (PDF). See DOI: 10.1039/x0xx00000x The crystallographic data files for the complexes have been deposited with the Cambridge Crystallographic Database as CCDC 2038629-2038634.

Polypyridines (phen and bpy) and their myriad derivatives are common ligands for half-sandwich complexes. Detailed solution behaviour and/or biological data were reported with Ru,[3,11-13] Rh,[14] Ir[14-16] and Os[16,17]. These ligands usually show similar or higher cytotoxic activity than their metal complexes.[12] However, complex formation in general might have advantageous effects on the selective cytotoxicity on cancer cells, since it can change the overall charge, lipophilicity and size, which affect the pharmacokinetics and can also result in altered mechanism of action. Different biological effects were found for Ru/Rh polypyridyl complexes. DNA intercalation was reported in the coordinatively saturated and kinetically inert tris-polypyridyl Ru and Rh complexes, in which mostly phen and its derivatives are the ligands.[18,19] On the other hand, taking into consideration the viscosity measurements, cytotoxicity data and ultrafiltration measurements, DNA-intercalation is not likely to occur and DNA is not believed to be the target molecule of half-sandwich complexes $[Ru/Rh(arene)(phen)(H_2O)]^{2+}$.[20-22] There are also examples for topoisomerase I and II inhibitors,[23] octahedral and half-sandwich cholinesterase inhibitors.[24]

In the field of cancer treatment, one of the major impediments is the appearance of resistance to chemotherapeutic agents. Cellular mechanisms promoting multidrug resistance (MDR) often rely on the elevated expression of ATP-binding cassette proteins, which pump a wide variety of drug molecules from the cell.[25-27] Drug resistant cells resort to further mechanisms in the case of compounds that are not recognized as transported substrates. In the case of cisplatin, cells become resistant as a result of elevated glutathione concentrations and increased DNA-repair.[26] Interestingly, the majority of RAED compounds seemed to overcome cisplatin resistance in the A2780cis cell lines model.[3] Similarly, a Ru cyclopentadienyl complex containing 4,4'-dimethyl-2,2'-bipyridine (dmb) showed comparable activity in parental and in cisplatin-resistant cancer cells.[28] In our former studies, we reported half-sandwich complexes with high stability, in which the ligands were 8-hydroxyquinoline derivatives.[29,30] The ligands substituted at the 7th position showed preferential toxicity in otherwise multidrug resistant MES-SA/Dx5 and Colo320 cell lines, and this characteristic persisted after combination with the half-sandwich organometallic $[Rh(\eta^5\text{-}C_5Me_5)(H_2O)_3]^{2+}$ triaqua cation.[29,30] However, complex formation with $[Ru(\eta^6\text{-arene})(H_2O)_3]^{2+}$ resulted in a decrease in cytotoxicity and the loss of preferential toxicity.[29,30]

In this study, we selected four polypyridines and their half-sandwich Ru and Rh complexes to reveal possible relationships between their structure, aqueous solution behaviour and anticancer activity against parental and drug resistant cancer cell lines. We synthesized novel Ru(η^6-toluene) to investigate the effects of the exchanges of *p*-cymene to toluene, and 2,9-dimethyl-1,10-phenanthroline (neocuproine, neo) complexes were also prepared to reveal the effect of methylation close to the coordinating nitrogens.

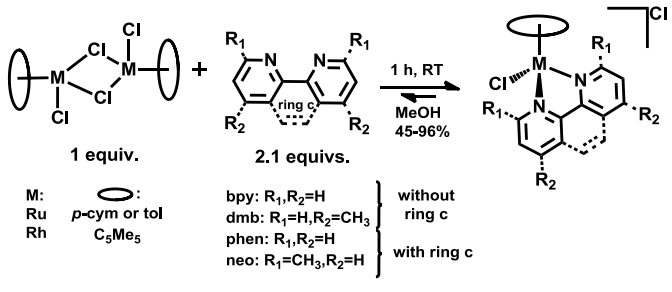

Scheme 1 Synthesis procedure of the complexes.

Results and discussions

Synthesis and characterization of complexes

As illustrated in Scheme 1, synthesis of complexes with the general formula [M(arene)(N,N)Cl]Cl, where M: Ru or Rh, arene: *p*-cymene (*p*-cym), toluene (tol), $C_5Me_5^-$, (N,N): bpy, dmb, phen and neo, was performed according to previously described methods.[11,31-33] Among the listed complexes, Ru(η^6-tol) complexes and neo complexes are new compounds. In this work, all the [M(arene)(N,N)Cl]Cl complexes were obtained as orange solids with moderate-to-excellent yields (45-95%) using methanol (MeOH) as solvent. Notably, the neo complexes were isolated in the lowest yields, which could be improved by using an excess of the ligand. [Ru(η^6-*p*-cym/tol)(ethylenediamine)Cl]Cl complexes are well-known compounds,[2] they were also synthesized with the same method for further solution chemical and comparative purposes.

^{1}H and ^{13}C NMR spectra recorded in CD_3OD confirmed complex formation, as shown in Figures S1-S14. Deuteration of the C_5Me_5 ligand (-CH_2D and -CHD_2 groups) was detected in the ^{1}H and ^{13}C NMR spectra, as three peaks are shown in Figure S7 with the same intensity next to the peak of the methyl groups. ESI-MS spectra were recorded only for the novel complexes, and the results confirmed the stoichiometry of each complex (Figures S15-S21).

Stability and photosensitivity of the complexes were investigated in water (at pH 7.4). Notably, the Rh complexes were stable in water for at least 7 days, as the yellow colour and the ^{1}H NMR spectra remained unchanged (see Figure S22 as an example). In order to investigate the photostability of the Ru complexes parallel samples of $[Ru(\eta^6\text{-tol})(bpy)(H_2O)]^{2+}$, $[Ru(\eta^6\text{-}p\text{-cym})(bpy)(H_2O)]^{2+}$ and $[Ru(\eta^6\text{-}p\text{-cym})(phen)(H_2O)]^{2+}$ were prepared and followed in time by UV-visible (UV-Vis) spectrophotometry. One of the parallel samples was protected from light, while the other was exposed to diffuse solar irradiation. The starting solutions had yellow colour, which is typical for half-sandwich complexes. Spectra of the complexes (shown in Figure S23) remained unchanged in dark after one day, except for $[Ru(\eta^6\text{-tol})(bpy)(H_2O)]^{2+}$, which showed signs of decomposition after 18 h (Figure S23.a). Namely, the sample turned blue-green, and a new band developed in the UV-visible (UV-Vis) spectra, first after 18 h with λ_{max} = 588 nm, and after 6 days another band appeared with λ_{max} = 644 nm. When exposed to light for a longer period of time, all samples showed signs of this process, which is most probably linked to the irreversible decomposition of the half-sandwich structure (also known as arene loss). The decomposition of $[Ru(\eta^6\text{-}p\text{-cym})(bpy)(H_2O)]^{2+}$ is slower than that of the toluene analogue, which appears only after more than 1 day. The product has the same λ_{max} at 588 nm (Figure S23.b), which is indicative of the loss of arene. The product of $[Ru(\eta^6\text{-}p\text{-cym})(phen)(H_2O)]^{2+}$ has a λ_{max} = 658 nm, where a tiny amount (A_{max}~0.03) appears only in light after 4 days (Figure S23.c). These experiments suggest that the

metal–carbon bond in the organometallic moiety can break and both the type of the metal ion and the arene have important roles in the stabilization: the bond between Ru(II) and *p*-cymene is more stable than between Ru(II) and toluene, while the bond between Rh(III) and $C_5Me_5^-$ is the strongest in this set of complexes. In case of Ru complexes formed with other (N,N) bidentate ligands, the loss of the arene ligand was reported earlier.[34] In our previous studies, arene loss induced by ligand excess or by another coordinating bidentate ligand was observed.[29,30] Stability studies of the bpy complexes was followed in the cell culture medium Roswell Park Memorial Institute Medium 1640 (RPMI 1640) completed with fetal bovine serum (FBS) in dark. Under these conditions no arene ligand dissociation was detected (Figure S24).

Reactions of the complexes in the cell culture medium Dulbecco's Modified Eagle Medium (DMEM) was also followed for a week by ^{1}H NMR spectroscopy. This medium provides physiological pH and contains inorganic salts, amino acids, sugar and vitamins, which may interact with these complexes. Figure S25 shows the important ranges of the recorded spectra, focused on the interactions with biomolecules. In the case of $[Rh(\eta^5\text{-}C_5Me_5)(phen)(H_2O)]^{2+}$ and $[Ru(\eta^6\text{-}p\text{-cym})(phen)(H_2O)]^{2+}$ complexes after 5 h new peaks appeared showing the formation of mixed ligand complexes. After this period, no big changes in the spectra could be observed after one week, except in the case of neo complexes, which showed a slow reaction and changed continuously. The complex of $[Ru(\eta^6\text{-}p\text{-cym})(neo)(H_2O)]^{2+}$ partially dissociated even in the phosphate buffer, indicating its lower stability at pH = 7.40. The measurements were repeated in RPMI 1640 medium completed with FBS (Figure S26). New sets of peaks were observed only for the $[Rh(\eta^5\text{-}C_5Me_5)(phen)(H_2O)]^{2+}$ complex compared to the spectra measured in DMEM.

The structures of (N,N) donor bidentate ligands complexes formed with $Ru(\eta^6\text{-arene})$ and $Rh(\eta^5\text{-}C_5Me_5)$ organometallic cations are well-known and several examples show the complexes in chlorinated[3,12,13,20] or in aqua form[35,36] in the solid structures. The different arene ligands did not change the piano-stool shaped structure. However, Ru–N and Ru–ring centroid distances can vary in these complexes. Generally, the structures represent mono complexes, in which the ligands are bound to the metal centre through two nitrogen atoms.

After counter ion exchange (Cl^- to CF_3SO_3), single crystals for complexes $[Rh(\eta^5\text{-}C_5Me_5)(dmb)Cl](CF_3SO_3)$ (crystal **I**), $[Ru(\eta^6\text{-tol})(dmb)Cl](CF_3SO_3)$ (crystal **II**) and $[Ru(dmb)_3](CF_3SO_3)_2{\times}2\ H_2O$ (crystal **III**) were obtained, which were subjected to X-ray crystallographic structure determination. Crystal data and structure refinement parameters are collected in Table S1. The results proved the presence of half-sandwich structure of the $[Rh(\eta^5\text{-}C_5Me_5)(dmb)Cl]^+$ and $[Ru(\eta^6\text{-tol})(dmb)Cl]^+$ complexes, similarly to the other $[Ru(\eta^{6/5}\text{-arene})(polypyridyl)Cl]^+$ complexes, *e.g.* $[Ru(\eta^6\text{-}p\text{-cym})(dmb)Cl]^+$.[37] However, a dark red crystal was also isolated that showed evidence of arene loss and the formation of $[Ru(dmb)_3](CF_3SO_3)_2{\times}2\ H_2O$ with octahedral structure. This irreversible reaction occurred in organic solvents and in water as well (*vide supra*), as the colour of solutions turned to green-blue over time. The $[Rh(\eta^5\text{-}C_5Me_5)(dmb)Cl](CF_3SO_3)$ complex crystallized

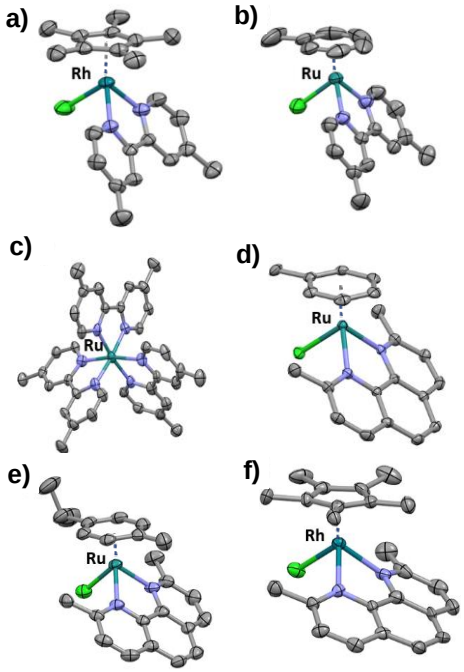

Fig. 1 Molecular structures of a) $[Rh(\eta^5\text{-}C_5Me_5)(dmb)Cl](CF_3SO_3)$ (**I**), b) $[Ru(\eta^6\text{-tol})(dmb)Cl](CF_3SO_3)$ (**II**) c) $[Ru(dmb)_3].2(CF_3SO_3){\times}2\ H_2O$ (**III**), d) $[Ru(\eta^6\text{-tol})(neo)Cl]Cl{\times}2$ MeOH (**IV**), e) $[Ru(\eta^6\text{-}p\text{-cym})(neo)Cl](CF_3SO_3)$ (**V**) and f) $[Rh(\eta^5\text{-}C_5Me_5)(neo)Cl](CF_3SO_3)$ (**VI**). Hydrogen atoms, solvent molecules and counter ions are omitted for clarity. Displacement ellipsoids are drawn at 50% probability level.

in the orthorhombic and both Ru complexes in the monoclinic crystal systems in *Pbcn*, $P2_1/n$ and $P2_1/c$ space groups, respectively, with the inclusion of a $CF_3SO_3^-$ counter ion (and two water molecules in the latter) per asymmetric unit. The ORTEP representation of the compounds is depicted in Figure 1.a,b,c.

Crystal structures of $[Ru(\eta^6\text{-tol})(neo)Cl]Cl{\times}2$ MeOH (crystal **IV**), $[Ru(\eta^6\text{-}p\text{-cym})(neo)Cl](CF_3SO_3)$ (crystal **V**) and $[Rh(\eta^5\text{-}C_5Me_5)(neo)Cl](CF_3SO_3)$ (crystal **VI**) could be also obtained (Figure 1.d,e,f). Crystal data and structure refinement parameters for neo complexes are collected in Table S2. Crystal **IV** and **V** crystallized in the monoclinic and crystal **VI** in the triclinic crystal systems in $P2_1/c$ (**IV, V**) and P-1 (**VI**) space groups. The asymmetric unit contains one complex and one counter ion in crystal **V**, two extra MeOH molecules in crystal **IV** and two complexes with two counter ions in crystal **VI**. Selected bond lengths and angles are collected in Tables S3-S4. In the the neo complexes, the neo ligand is not fully planar. The angle enclosed by the planes of the outer ring is bended for **IV** and **V** (12.7° and 9.8°, respectively) and the most bent ring was found in crystal **VI** where this angle is 17.2° and 17.7° for molecules 1 and 2. The bar chart in Figure S27 shows the metal ion–N atom distances, which are longer for neo complexes and are the shortest in the tris-dmb complex.

The structures of $[Ru(\eta^6\text{-tol})(dmb)Cl](CF_3SO_3)$ and $[Ru(\eta^6\text{-}p\text{-cym})(dmb)Cl](BF_4)$[37] are practically identical as the average Ru–N bond lengths are 2.088 Å vs. 2.085 Å, the Ru–ring centroid distances are 1.686 Å vs. 1.685 Å. The two Ru complexes of neo also show a strong similarity, the change of arene has no effect on the

geometrical parameters (Figure S28.a). The geometrical changes are negligible when *p*-cymene is substituted to toluene ligand.

All neocuproine containing structures differ from the analogous phen complexes,[13,20] as the steric congestion around the metal ion is caused by the methyl groups in the 2nd and 9th positions. For instance the Rh−N bond length changed from 2.11 Å to 2.13 Å, in case of exchanges of phen to neo change. A spectacular proof of the steric hindrance is the finding that the planes of the arene ligand and of the bidentate ligand are not the same. The difference between $[Ru(\eta^6\text{-}p\text{-cym})(neo)Cl]^+$ and $[Ru(\eta^6\text{-}p\text{-cym})(phen)Cl]^+$ complexes is shown in Figure S28.b.[13] In this example there is a 19° alteration between the plane of phen and neo. The best visualization for this steric congestion is provided by the ligand solid angles calculated by the Olex2 software.[38,39] Figure S29 shows the ligand solid angles in the complex of $[Ru(\eta^6\text{-}p\text{-cym})(neo)Cl]^+$, from two different views. Less overlap is present between the ligands around Rh(III) than in the two Ru(II) complexes (see more details in the legend of Figure S29). For crystallization of all neocuproine complexes we also tried to perform anion exchange using $Ag(CF_3SO_3)$ salt. However, during the crystallization procedure, red crystals of the precursor $[M(arene)Cl_2]_2$ dimer and colourless crystals of $[Ag(neo)_2](CF_3SO_3)$ appeared in these samples, most probably as a consequence of the low stability of the neocuproine complexes (notably they were also characterized by the lowest yields in synthesis). Scheme S1 shows side reactions of neocuproine complexes.

In vitro anticancer activity

The anticancer activity of four related polypyridyl ligands (phen, neo, bpy, dmb) and their half-sandwich $Ru(\eta^6\text{-}p\text{-cym})$, $Ru(\eta^6\text{-tol})$ and $Rh(\eta^5\text{-}C_5Me_5)$ complexes was investigated against the uterine sarcoma cell line MES-SA and its doxorubicin resistant counterpart MES-SA/Dx5, as well as against the ovarian cancer cell line A2780 and its cisplatin resistant counterpart A2780cis. A2780cis cells show an increased ability to repair DNA and have higher intracellular concentrations of glutathione,[26] while MES-SA/Dx5 cells overexpress P-gp,[26,40] which results in multidrug resistance.

The paradoxical toxicity of phen against P-glycoprotein (P-gp)-expressing MDR cells (MDR-selective toxicity) was reported earlier.[41] A summary of the literature data on the *in vitro* toxicity of the half-sandwich complexes of the selected ligands on other cancer cell lines is shown in the Electronic Supplementary Information.[13,14,42,43]

The obtained IC_{50} values are shown in Tables 1-2 and in Figure S30. The relative toxicity of the complexes against parental and drug resistant cancer cell lines was compared, and the selective toxicity was expressed as resistance ratio (RR = IC_{50} (resistant cell) / IC_{50} (sensitive cell)). Based on the determined IC_{50} values (Tables 1-2), the ligands phen, neo and dmb displayed significant toxicity, reaching submicromolar IC_{50} values in some cases. Neocuproine has a superior cytotoxic effect, it is comparable with doxorubicin (and 10 times higher than phen) in MES-SA cells, while 20 times more active than cisplatin in A2780 cells. The toxicity of the $[Rh(\eta^5\text{-}C_5Me_5)(N,N)Cl]^+$ complexes were similar or slightly lower compared to that of their corresponding ligands. Surprisingly, the Ru complexes exhibited in all cases weaker cytotoxicity than the Rh congeners.

Table 1 *In vitro* cytotoxic effects (72 h) (IC_{50} values in μM) in parental (MES-SA) and multidrug resistant (MES-SA/Dx5) cell lines treated with polypyridine ligands and their half-sandwich complexes in addition to the corresponding organometallic precursors. Resistance ratio (RR = IC_{50}(MES-SA/Dx5)/IC_{50}(MES-SA)) values are also represented. N. d. = not determined (in cases where both IC_{50} > 100 μM).

	MES-SA	MES-SA/Dx5	RR
phen	4 ± 1	1.30 ± 0.01	0.33
$[Rh(\eta^5\text{-}C_5Me_5)(phen)Cl]Cl$	8 ± 2	2.0 ± 0.9	0.25
$[Ru(\eta^6\text{-tol})(phen)Cl]Cl$	> 100	> 100	n. d.
$[Ru(\eta^6\text{-}p\text{-cym})(phen)Cl]Cl$	24 ± 12	> 100	>4.2
neo	0.37 ± 0.08	0.30 ± 0.04	0.81
$[Rh(\eta^5\text{-}C_5Me_5)(neo)Cl]Cl$	1.4 ± 0.1	2.66 ± 0.09	1.90
$[Ru(\eta^6\text{-tol})(neo)Cl]Cl$	2.1 ± 0.2	4.2 ± 0.7	2.00
$[Ru(\eta^6\text{-}p\text{-cym})(neo)Cl]Cl$	4 ± 1	7 ± 1	1.75
bpy	66 ± 19	50 ± 15	0.75
$[Rh(\eta^5\text{-}C_5Me_5)(bpy)Cl]Cl$	> 100	69 ± 25	<0.7
$[Ru(\eta^6\text{-tol})(bpy)Cl]Cl$	> 100	> 100	n. d.
$[Ru(\eta^6\text{-}p\text{-cym})(bpy)Cl]Cl$	> 100	> 100	n. d.
dmb	46 ± 7	15 ± 2	0.33
$[Rh(\eta^5\text{-}C_5Me_5)(dmb)Cl]+$	41 ± 6	16 ± 6	0.39
$[Ru(\eta^6\text{-tol})(dmb)Cl]+$	> 100	> 100	n. d.
$[Ru(\eta^6\text{-}p\text{-cym})(dmb)Cl]+$	63 ± 11	> 100	>1.59
$[Rh(\eta^5\text{-}C_5Me_5)Cl2]2$	> 100	> 100	n. d.
$[Ru(\eta^6\text{-tol})Cl2]2$	> 100	> 100	n. d.
$[Ru(\eta^6\text{-}p\text{-cym})Cl2]2$	> 100	> 100	n. d.
doxorubicin	0.35 ± 0.06	3 ± 0.9	8.57

Table 2 *In vitro* cytotoxic effect (72 h) (IC_{50} values in μM) of polypyridine ligands and their half-sandwich complexes in addition to the organometallic precursors in sensitive (A2780) and cisplatin resistant (A2780cis) human ovarian cancer cell lines. Resistance ratio (RR = IC_{50}(A2780cis)/IC_{50}(A2780)) values are also represented. N. d. = not determined (in cases where both IC_{50} > 100 μM).

	A2780	A2780cis	RR
phen	0.14 ± 0.03	2.5 ± 0.2	17.9
$[Rh(\eta^5\text{-}C_5Me_5)(phen)Cl]Cl$	0.28 ± 0.09	10 ± 3	35.7
$[Ru(\eta^6\text{-tol})(phen)Cl]Cl$	38 ± 12	> 100	>2.6
$[Ru(\eta^6\text{-}p\text{-cym})(phen)Cl]Cl$	11 ± 2	> 100	>9.1
neo	0.13 ± 0.03	9 ± 2	69.2
$[Rh(\eta^5\text{-}C_5Me_5)(neo)Cl]Cl$	0.4 ± 0.2	1.2 ± 0.3	3.0
$[Ru(\eta^6\text{-tol})(neo)Cl]Cl$	0.6 ± 0.1	1.5 ± 0.3	2.5
$[Ru(\eta^6\text{-}p\text{-cym})(neo)Cl]Cl$	2 ± 1	6 ± 4	3.0
bpy	2.4 ± 0.8	39 ± 20	16.3
$[Rh(\eta^5\text{-}C_5Me_5)(bpy)Cl]Cl$	7 ± 3	> 100	>14.3
$[Ru(\eta^6\text{-tol})(bpy)Cl]Cl$	11.2 ± 0.9	> 100	>8.9
$[Ru(\eta^6\text{-}p\text{-cym})(bpy)Cl]Cl$	19 ± 5	> 100	>5.3
dmb	0.13 ± 0.07	35 ± 6	269
$[Rh(\eta^5\text{-}C_5Me_5)(dmb)Cl]+$	0.4 ± 0.2	57 ± 10	143
$[Ru(\eta^6\text{-tol})(dmb)Cl]+$	~100	> 100	>1.0
$[Ru(\eta^6\text{-}p\text{-cym})(dmb)Cl]+$	13 ± 3	57 ± 9	4.4
$[Rh(\eta^5\text{-}C_5Me_5)Cl2]2$	45 ± 6	> 100	>2.2
$[Ru(\eta^6\text{-tol})Cl2]2$	> 100	> 100	n. d.

[Ru(η^6-*p*-cym)Cl2]2	> 100	> 100	n. d.
cisplatin	2.5 ± 0.8	17 ± 8	6.8

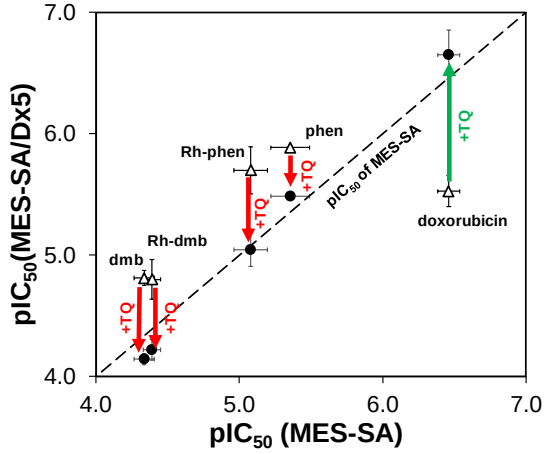

Fig. 2 Effect of the P-gp inhibitor TQ on pIC_{50} values in MES-SA and MES-SA/Dx5 cells. Doxorubicin and compounds with paradoxical cytotoxicity are shown. 'Rh-dmb' and 'Rh-phen' represent the corresponding $[Rh(\eta^5\text{-}C_5Me_5)(N,N)(H_2O)]^{2+}$ complexes. Points above the diagonal represent paradoxical behaviour; points on the diagonal show compounds, whose cytotoxic effect is the same on both cell lines; points under the diagonal display lower toxicity in MES-SA/Dx5 than in MES-SA. △: without TQ; ●: co-incubated with TQ. Arrows show the effect of TQ on the activity, which is decreased in the case of compounds with paradoxical toxicity (red) potentiated by P-gp, while increased for non-selective compounds (green).

As compared to A2780 parental cells, the cisplatin-resistant A2780cis cells were found to be cross-resistant to all investigated compounds (*c.f.* IC_{50} values in Table 2). However, the RR values are smaller for the neocuproine complexes unlike the ligand or the cisplatin itself. Interestingly, ligands phen, dmb and their Rh complexes showed higher cytotoxicity in MES-SA/Dx5 cell lines than in the MES-SA cells (RR < 0.5 in Table 1), suggesting that these compounds may show MDR-selective activity.[25] However, despite the similar structures of neo and phen or bpy and dmb, neo and bpy showed no preferential toxicity against MES-SA/Dx5 cells. The toxicity of MDR-selective compounds is exacerbated by the function of P-gp.[41,44]

To test the relevance of P-gp function in the selective toxicity of phen, dmb and their Rh complexes, the *in vitro* toxicity assays were repeated in the presence of the P-gp inhibitor tariquidar (TQ) in MES-SA and MES-SA/Dx5 cell lines (Figure 2, Table S5). As expected, the IC_{50} of doxorubicin significantly decreased (pIC_{50} increased), in line with the inhibition of drug efflux. In contrast, phen, dmb and their Rh complexes show decreased toxicity in the presence of TQ, proving that their activity is potentiated by P-gp. The most prominent example is dmb, where the IC_{50} in MES-SA/Dx5 cells changes from 15 μM to 72 μM upon addition of TQ, respectively.

As a conclusion, phen, dmb and their Rh complexes were found to be cytotoxic, and showed preferential cytotoxicity in the MES-SA/Dx5 cell-line. Exchange of Rh to Ru results in the loss of activity and selectivity, as it was found in our previous publications for ligands with (N,O) donor set.[29,30] In line with the results reported for these 8-hydroxyquinoline complexes[14,15] irreversible arene loss was found for Ru complexes, and a somewhat higher cell accumulation was detected in the case of Rh. These findings might contribute to the different anticancer properties of the Ru and Rh polipyridyl complexes as well. In case of the Ru complexes, which were characterized in this work, arene loss was demonstrated even without an extra ligand (*vide supra*), which might be responsible for the observed loss of cytotoxicity in parental and/or resistant cell lines. Since the methylation of ligands (phen and bpy to neo and dmb), and the type of the metal centre (Ru or Rh) strongly affect the toxicity in the MES-SA and the MDR counterpart MES-SA/Dx5 cell lines, further studies were performed in order to better understand the differences in the solution behaviour of these complexes. The A2780cis cells showed cross-resistance for these compounds, however, cells were less cross-resistant for the complexes of neocuproine, as the RR values indicate.

Deprotonation of ligands and hydrolysis of half-sandwich cations

Hydrolysis of the organometallic cations and the protonation constants of the ligands influence the solution speciation of metal complexes. The hydrolytic processes of half-sandwich cations ($[Rh(\eta^5\text{-}C_5Me_5)(H_2O)_3]^{2+}$, $[Ru(\eta^6\text{-}p\text{-cym})(H_2O)_3]^{2+}$ and $[Ru(\eta^6\text{-tol})(H_2O)_3]^{2+}$) were already investigated in detail earlier.[45,46] Proton dissociation constants of bpy, phen and ethylenediamine (Table 3) are also known under various conditions,[47,48] and were re-determined herein by pH-potentiometry (see detailed description of this method in ESI). Due to the limited water solubility of dmb and neo, only spectrophotometric titrations were feasible for these ligands in chloride-free medium (I = 0.20 M KNO_3) using lower concentrations.

Table 3 Proton dissociation constants (K_a (H_2L) and K_a (HL)) for (N,N) ligands, stability (K [M(arene)(L)]), proton dissociation (K_a [M(arene)(L)]) and water-chloride exchange (K' (H_2O/Cl^-)) constants of complexes of phen, neo, bpy, dmb and en. {T = 25.0 °C; I = 0.20 M (KNO_3)}

M(arene)	Constant	phen	neo	bpy	dmb	en
	pK_a(HL)	4.92[a]	5.77(1)	4.41[b]	5.31(1)	H_2L: 7.25, HL: 10.01[b]
Rh(η^5-C_5Me_5)	log K [M(arene)(L)]	14.70(3)[c]	9.70(3)[d]	13.30(2)[c]	14.32(2)[c]	15.04[b]
	pK_a [M(arene)(L)]	8.58[a]	8.88(1)[e]	8.61[b]	8.40(1)[f]	9.58[b]
	log K' (H_2O/Cl^-)	2.92[a]	2.76(1)[g]	2.58[b]	2.36(1)[g]	2.14[b]
Ru(η^6-*p*-cym)	log K [M(arene)(L)]	>12.8	8.21(4)[e]	>12.5	>12.8	14.85(5)[h]
	pK_a [M(arene)(L)]	7.59(1)[f]	7.62(1)[e]	7.48(1)[f]	7.55(1)[f]	8.14(2)[e]
	log K' (H_2O/Cl^-)	1.79(1)[g]	0.93(1)[g]	1.83(1)[g]	2.02(1)[g]	1.51(5)[g]
Ru(η^6-tol)	log K [M(arene)(L)]	>13.0	8.19(8)[e]	>13.0	>13.2	14.90(6)[h]
	pK_a [M(arene)(L)]	7.39(1)[f]	7.55(1)[e]	7.39(1)[f]	7.47(1)[f]	8.04(2)[e]
	log K' (H_2O/Cl^-)	1.68(1)[g]	0.87(1)[g]	1.62(1)[g]	1.88(1)[g]	1.69(5)[g]

[a] See Ref. 22. [b] See Ref. 49. [c] ^{1}H NMR, displacement measurements. [d] ^{1}H NMR, pH = 0.7-2.1. [e] ^{1}H NMR titrations, pH = 2.0-11.5. [f] UV-Vis titration, pH = 2-11.5. [g] UV-Vis, *c*(Cl^-)=0.0-0.2 M. [h] ^{1}H NMR, *c*(M(arene)) = 100 μM, *c*(ethylenediamine) = 0-7.3 mM.

Considering the different ionic strengths, values are in good agreement with literature data.[47,48] We find that methylation in ortho and in para positions increases the pK_a. Based on the pK_a values it can be concluded that the polypyridyl ligands are mainly in their neutral form at physiological pH.

Determination of formation constants for complexes $[M(arene)(N,N)(H_2O)]^{2+}$

Based on the single-crystal X-ray structures and previous solution equilibrium studies on similar complexes,[3,13,22,49] these bidentate (N,N) donor ligands form mono complexes with half-sandwich organometallic triaqua cations. Scheme S2 shows the occurring equilibrium processes in aqueous solutions for these complexes. Although the complex formation equilibrium is reached with (O,O) donors within minutes, hours or days are needed in case of the (N,N) donors.[22] Complex formation rates at pH = 0.7 and 2.1 are compared in Figures S31-S33, which show that the $[Ru(\eta^6\text{-arene})(H_2O)_3]^{2+}$ triaqua cations react much slower than $[Rh(\eta^5\text{-}C_5Me_5)(H_2O)_3]^{2+}$ with the same ligand (h *versus* min). Generally, it can be concluded that the reaction rate is lower at more acidic pH. However, the pH cannot be increased beyond a certain limit to accelerate the reaction, since the hydrolysis of the organometallic cations produces inert hydroxido complexes.

Complexes of bpy, dmb and phen are present in aqueous solutions at pH = 2 and 0.7 exclusively, there is no sign of unbound organometallic cation or ligand under the given conditions (*I* = 0.20 M KNO_3, aqueous solution) based on the ^{1}H NMR spectroscopic measurements. (Notably, pH 0.7 is the lowest pH where the ionic strength can be kept constant.) With decreasing concentrations (from 1.2 mM to 20 μM) of $[Ru(\eta^6\text{-tol})(bpy)(H_2O)]^{2+}$ and $[Ru(\eta^6\text{-}p\text{-cym})(phen)(H_2O)]^{2+}$, the molar UV-Vis spectra remain unchanged (Figure S34), which also confirmed the high stability of the complexes. Since measurements with decreasing pH (down to 0.7) or concentration (down to 20 μM) do not give any information about the stability constants owing to the lack of complex dissociation, displacement studies were performed with ethylenediamine. For this purpose, stability constants for $[Ru(\eta^6\text{-arene})(ethylenediamine)(H_2O)]^{2+}$ were determined (the constant of $[Rh(\eta^5\text{-}C_5Me_5)(ethylenediamine)(H_2O)]^{2+}$ was reported earlier).[49] Samples were prepared at pH = 3.0 using different ethylenediamine-to-Ru ratios (up to 14-fold ligand excess) and measured by ^{1}H NMR spectroscopy. Figure S35 shows extremely slow complex formation under the conditions used.

When ~80-fold excess of ethylenediamine was used, signals of mixed ligand complexes appeared in the ^{1}H NMR spectra instead of the free polypyridine ligand. Figure S36 shows examples for $[Rh(\eta^5\text{-}C_5Me_5)(bpy)(H_2O)]^{2+}$ – ethylenediamine and $[Ru(\eta^6\text{-tol})(bpy)(H_2O)]^{2+}$ systems, in which two peaks indicated the monodentate coordination of ethylenediamine. This ternary complex formation process hindered the determination of the stability constant.

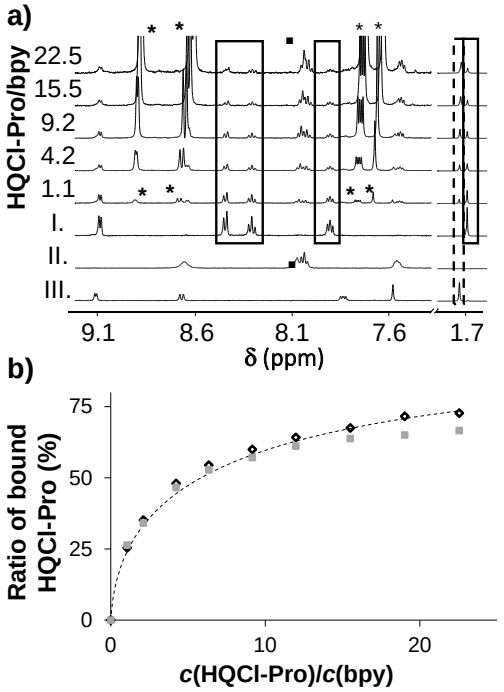

Fig. 3 a) Selected ^{1}H NMR spectra of the $[Rh(\eta^5\text{-}C_5Me_5)(bpy)(H_2O)]^{2+}$-HQCl-Pro (1:x) system at different HQCl-Pro concentrations (x = 0-22.5). Intensity is decreased in δ < 2.0 ppm region for the sake of clarity. I.: spectrum of $[Rh(\eta^5\text{-}C_5Me_5)(bpy)(H_2O)]^{2+}$; II.: spectrum of unbound bpy at pH 6.19; III.: spectrum of $[Rh(\eta^5\text{-}C_5Me_5)(L)(H_2O)]^{+}$, where L is the deprotonated (coordinated) form of HQCl-Pro. Peaks signed with * belong to the unbound HQCl-Pro; ■ shows the peak of bpy used for calculations; dashed rectangle shows $[Rh(\eta^5\text{-}C_5Me_5)(L)(H_2O)]^{+}$; solid rectangle shows $[Rh(\eta^5\text{-}C_5Me_5)(bpy)(H_2O)]^{2+}$. b) Measured and fitted (dashed line) percentages of $[Rh(\eta^5\text{-}C_5Me_5)(L)(H_2O)]^{+}$; ■ is calculated from integrals of unbound-bound bpy peaks, ◊ is calculated from C_5Me_5 peaks. {*c*($[Rh(\eta^5\text{-}C_5Me_5)(H_2O)_3]^{2+}$) = *c*(bpy) = 200 μM; *c*(HQCl-Pro) = 0-4.53 mM; pH = 6.51; solvent: 90% H_2O / 10% D_2O; *T* = 25.0 °C; *I* = 0.20 M (KNO_3)}

An 8-hydroxyquinoline derivate ((*S*)-5-chloro-7-((proline-1-yl)methyl)8-hydroxyquinoline (HQCl-Pro))[30] was used for the competition experiments, however, its use was limited only to the Rh-containing compounds, as the Ru complexes seem to lose the arene ligands when a competitor ligand is added. A successful displacement of bpy from its Rh complex is shown in Figure 3, at 22.5-fold excess of HQCl-Pro ~70% of the liberated bpy. From this data a log *K* = 13.30(2) was calculated (Table 3). Bpy was employed for the displacement of dmb and phen ligands. In these measurements ^{1}H NMR spectroscopy was used, since the peak separation of these similar compounds is satisfactory on NMR spectra (Figures S37 and S38). To determine the stability constants of the Ru complexes, we attempted to study a potential displacement between the organometallic cations. Unfortunately, there was no reaction between $[Rh(\eta^5\text{-}C_5Me_5)(polypyridine)(H_2O)]^{2+}$ and $[Ru(\eta^6\text{-}p\text{-cym})(H_2O)_3]^{2+}$, even at 10-fold excess of the latter. In all, only minimum values could be provided (Table 3).

The behaviour of neocuproine complexes is different due to the steric effect of the methyl groups next to the donor atoms, namely the complex formation reaction is much slower as compared with phen. Samples containing $[Ru(\eta^6\text{-arene})(H_2O)_3]^{2+}$ and neocuproine in 1:1.2 ratio were followed by ^{1}H NMR spectroscopy for 15 days (Figure 4.a). An extra set of peaks belongs to an intermediate complex which is most probably a sandwich-type complex is (Figure 4.b,c). The solution stability of metal complexes also changed compared to phen. Free neocuproine occurs next to its Rh complex (pH = 0.7, ~50%, Figure S39.a) in the equilibrium, as well as next to the Ru complexes (pH = 2.5, ~15%, Figures 5.a and S40.a). Based on the samples measured for samples with acidic pH, molar fractions for bound and unbound neocuproine can be calculated and used for the determination of stability constants (Figure S39 shows this in case of Rh). The Ru-containing complexes have smaller stability constants (Table 3). The lower complex stability constants and the stronger bias of $[Ru(arene)(H_2O)_3]^{2+}$ towards hydrolysis ensure the lower aqueous stability of $[Ru(arene)(neo)(H_2O)]^{2+}$ complexes compared to $[Rh(\eta^5\text{-}C_5Me_5)(H_2O)_3]^{2+}$. The lower stability may originate from the shorter distance between the Ru metal ion and arene ligand compared with the Rh–C_5Me_5 distance (1.697 Å *vs.* 1.780 Å), which may cause greater steric repulsion around the Ru centre. To quantify this steric repulsion, the overlaps between ligand solid angles (calculated by Olex2[38]) were listed in the legend of Figure S29. The bigger the overlap, the less the aqueous stability of complex.

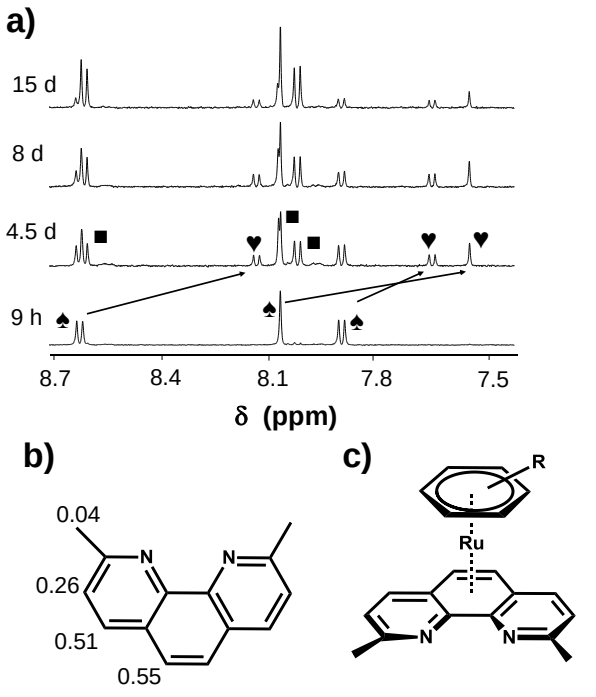

Fig. 4 a) Time-dependence of complex formation of $[Ru(\eta^6\text{-tol})(H_2O)_3]^{2+}$ with neo at pH = 6.0 followed by ^{1}H NMR spectroscopy (only region of ligand is shown). Time of reaction is shown on the left. Assignment: bidentate metal complex: ■, free neo: ♠, 'sandwich intermediate': ♥. Arrows show the unusually big shifts of 'sandwich intermediate' from free ligand, which differences are shown in b) (in ppm). c) Proposed structure of the 'sandwich intermediate'. {$c([Ru(\eta^6\text{-tol})(H_2O)_3]^{2+})$ = 200 μM; c(neo) = 245 μM; pH= 6.0 (20 mM phosphate); I = 0.20 M (KNO_3); T = 25.0°C}

Comparison of the stability constants of Rh complexes is not feasible due to the different basicity of the ligands. The derived stability constants are calculated as the equation shows below:

$$\log K^* = \log K\,[M(arene)(L)(H_2O)]^{2+} - pK_a(HL)$$

With this transformation, the log K^* $[Rh(\eta^5\text{-}C_5Me_5)(N,N)(H_2O)]^{2+}$ values show the following trend: 9.78 (phen) > 9.01 (dmb) > 8.89 (bpy) > 3.93 (neo). While methylation far from the coordinating nitrogen atoms (bpy *vs.* dmb) causes slight difference, the methylation next to the coordinating nitrogen atoms results in a huge difference. However, except neocuproine, there are no significant differences in the stability of these Rh complexes. The loss of preferential cytotoxicity in MES-SA/Dx5 cells of $[Rh(\eta^5\text{-}C_5Me_5)(neo)(H_2O)]^{2+}$ can be partly explained by the probable dissociation of neo-complex in the cell. However, the small stability difference between bpy and dmb cannot be the reason of the different behaviour against MDR cell lines. Moreover, the question arises whether the reactivity of the coordinated water molecule can be tuned using steric control of a bulky bidentate ligand.

Reactions of the coordinated water molecule: deprotonation and substitution to chloride ion

In half-sandwich complexes, next to the arene hapto ligand and a bidentate (N,N) donor ligand, the coordination sphere is completed by a water molecule, which can either lose a proton or can be substituted by another ligand (for example Cl^- in Scheme S2). Chen and co-workers found that the reaction of RAED complexes with nucleobases is slower at higher pH or in the presence of chloride or phosphate anions.[50] At higher pH, deprotonation occurs, which is characterized by the pK_a[M(arene)(L)] constant. With the knowledge of pK_a values one can calculate not only the actual average charge (between +2 and +1) of the compound at a given pH, which has an effect also on lipophilicity, but also the molar fraction of the generally less reactive $[M(arene)(L)(OH)]^+$ mixed hydroxido complex.

Increasing the pH, the effect of the deprotonation process on the UV-Vis spectra is unambiguous, as the pH-dependent spectra (Figure 5) of the example ($[Ru(\eta^6\text{-tol})(dmb)(H_2O)]^{2+}$) shows. From the absorbance change pK_a values can be computed. Determination of this constant is also feasible by performing ^{1}H NMR titrations, where the changes of the chemical shifts are used for calculations. In a previously reported article the pK_a of $[Ru(\eta^6\text{-}p\text{-cym})(phen)(H_2O)]^{2+}$ was determined as 7.32 in pure D_2O,[42] which is in good agreement with the constant reported here. This type of measurement was used in the case of $[Ru(\eta^6\text{-}p\text{-cym})(neo)(H_2O)]^{2+}$ and interestingly, in the region of aromatic *p*-cymene protons a singlet appears, which belongs to the arene in the complex (Figure 6). This peak belongs to protons, which are generally not magnetically equivalent in other complexes. As the pH increases, this singlet splits into two doublets.

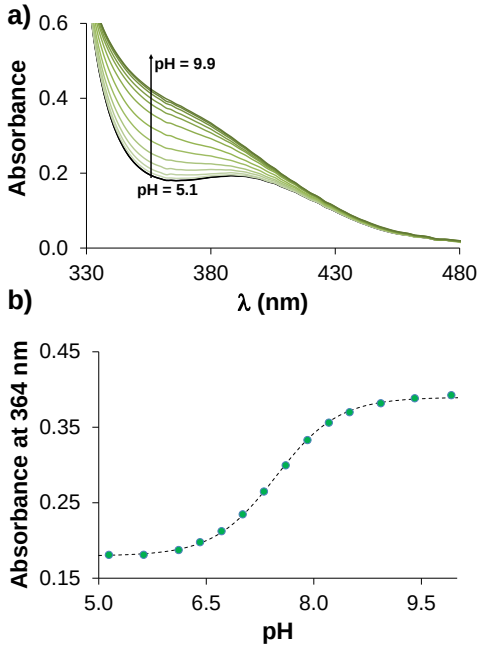

Fig. 5 a) UV-Vis spectra of the $[Ru(\eta^6\text{-tol})(dmb)(H_2O)]^{2+}$ recorded at pH = 5.1-9.9. b) Absorbance change at 364 nm in dependence of the pH. {$c([Ru(\eta^6\text{-tol})(dmb)(H_2O)]^{2+})$ = c(dmb) = 200 μM; I = 0.20 M (KNO_3); ℓ = 1 cm; T=25.0°C}

As shown in Table 3, methylation of the polypyridine ligands has an influence on the deprotonation of the coordinated water molecule. Namely, the methyl groups increase the pK_a values of the complexes in all cases. Ru complexes have stronger OH^- affinity than the Rh analogues, as the lower pK_a values indicate it. Due to the lower complex stability, at physiological pH $[(Ru(arene))_2(OH)_3]^+$ also appears in the case of $[Ru(arene)(neo)(H_2O)]^{2+}$ complexes.

Chloride ions can potentially replace the coordinating water molecule, as shown in the single-crystal XRD structures (Figure 1), and this process is characterized by the water-chloride exchange constant ($K'(H_2O/Cl^-)$). Cl^- is present in aqueous solutions, *e.g.* in biofluids, where the concentration drops from 103 mM to 24 mM and 4 mM, entering from the blood serum to cytoplasm and nucleus.[51] The coordination of Cl^- affects the actual charge and the presence of chloride ion in medium can suppress the deprotonation process of the complexes to a more basic pH region.[49] The Cl^- affinity of $[Rh(\eta^5\text{-}C_5Me_5)(phen)(H_2O)]^{2+}$ and $[Rh(\eta^5\text{-}C_5Me_5)(bpy)(H_2O)]^{2+}$ was already reported by our group.[22,49] Upon addition of chloride ions, changes similar to deprotonation can be observed in the UV-Vis spectra (as shown for $[Ru(\eta^6\text{-tol})(phen)(H_2O)]^{2+}$ in Figure 7.a). From the spectral changes the water-chloride exchange constants were calculated (Table 3). Methylation of the ligands has an effect on the water-chloride exchange constant as well. While for Rh complexes only a slight decrease can be seen, the effect for Ru complexes is remarkable. The Cl^- affinity of dmb complexes is higher than that of the bpy complexes. The Ru(II)-arene complexes of neocuproine have significantly low constants: log $K'(H_2O/Cl^-)$ = 1.79→0.93 and 1.68→0.87 (Table 3). The Cl^--dependent spectra of $[Ru(\eta^6\text{-}p\text{-cym})(neo)(H_2O)]^{2+}$ show smaller spectral changes (ΔA~0.05) in

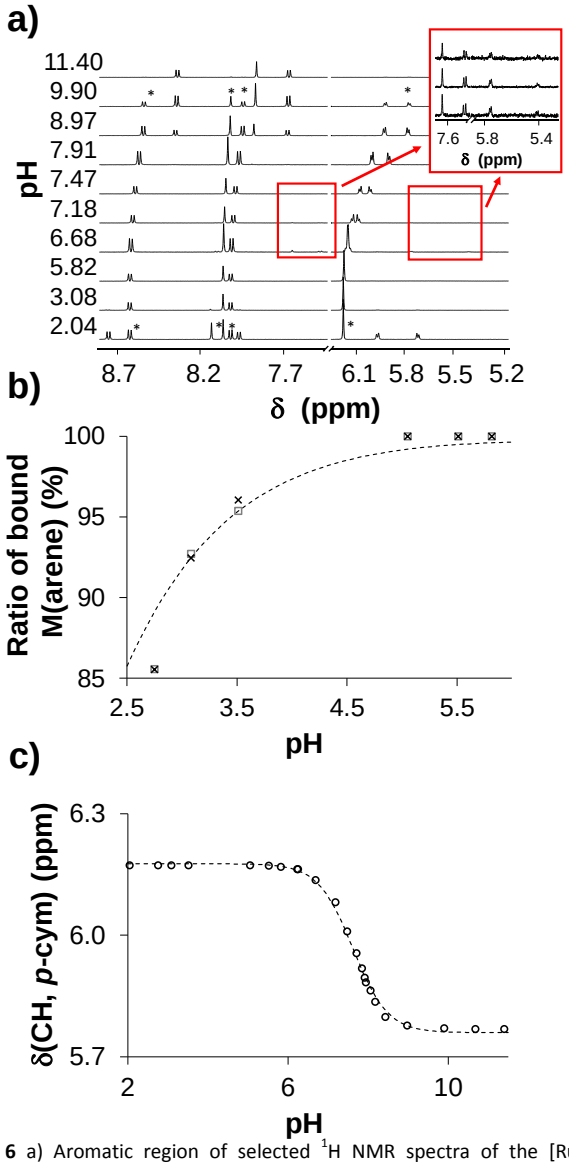

Fig. 6 a) Aromatic region of selected ^{1}H NMR spectra of the $[Ru(\eta^6\text{-}p\text{-cym})(neo)(H_2O)]^{2+}$ system recorded at pH = 2.0-11.4 after 34 days. Peaks of complex I are signed with *. Appearance of 'sandwich intermediate' is shown in the inset. b) Measured (neo H at position 5 and 6: □; all protons of ligand: ×) and fitted (dashed line) ratio of formed complex. c) Measured (○) and fitted (dashed line) chemical shift values of aromatic *p*-cymene protons at different pH-values. {$c([Ru(\eta^6\text{-}p\text{-cym})(H_2O)_3]^{2+})$ = c(neo) = 500 μM; solvent: 90% H_2O / 10% D_2O; T = 25.0°C; I = 0.20 M (KNO_3); c(phosphate) = 20 mM}

Figure S40.b. Most probably a steric repulsion is the reason. The methyl groups of neo hinder the strong interaction between the chloride ion and Ru.

For $[Ru(arene)(ethylenediamine)(H_2O)]^{2+}$ complexes, a larger uncertainty can be seen in the constants. This is in connection with the phosphate ion coordination to RAED complexes based on the

abovementioned work of Chen *et al.*,[50] and on our measurements showed in details in Figures S41-S42.

Figure 7.c shows the ratio of chlorinated and aqua forms of complexes in the solution at different chloride ion concentrations.

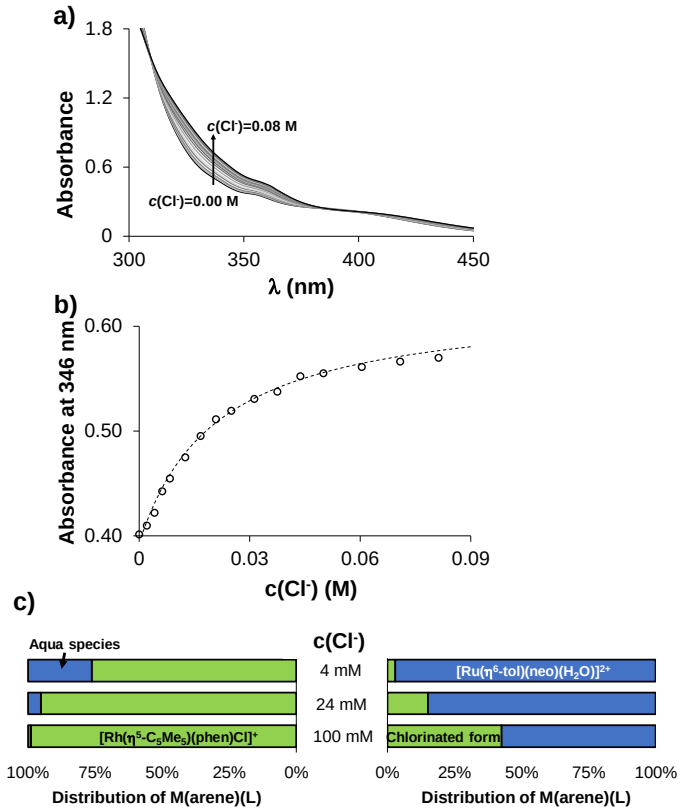

Fig. 7 a) UV-Vis spectra of $[Ru(\eta^6\text{-tol})(phen)(H_2O)]^{2+}$ recorded at various chloride ion concentrations. b) Absorbance change at 346 nm plotted against the concentration of the chloride ion. c) Ratio of the aqua and chlorinated forms of complexes (c = 200 μM) with the highest and lowest chloride affinity measured in the studied group of compounds. Chloride concentrations are representing the different biofluids. Constants from Table 3 were used for calculation. {$c([Ru(\eta^6\text{-tol})(H_2O)_3]^{2+}$) = c(phen) = 182 μM; pH = 6.0; ℓ = 1 cm; T = 25.0°C}

Our calculations show the contrasting behaviour of two complexes, which possess the highest and the lowest chloride ion affinity ($[Rh(\eta^5\text{-}C_5Me_5)(phen)(H_2O)]^{2+}$ and $[Ru(\eta^6\text{-tol})(neo)(H_2O)]^{2+}$, respectively). As seen in Figure 7.c, the fraction of the chlorinated form of the neo complex is minimal at $c(Cl^-)$ = 4 mM, and it increases to 43% at $c(Cl^-)$ = 100 mM. On the contrary, the $[Rh(\eta^5\text{-}C_5Me_5)(phen)(H_2O)]^{2+}$ complex shows an opposite behaviour, as the chlorinated form predominates under all considered chloride ion concentrations.

The importance of the knowledge of chloride ion affinity was already mentioned above and in previous reviews.[51] In our earlier work, a linear relationship between the pK_a[M(arene)(L)] and the log $K'(H_2O/Cl^-)$ constants was found for $Rh(\eta^5\text{-}C_5Me_5)$ complexes with (O,O), (O,N), (N,N) and (O,S) donor bidentate ligands. To complete this model, already published and the newly determined constants even for Ru(arene) complexes were integrated (except for neo complexes because of the strong steric effect on this

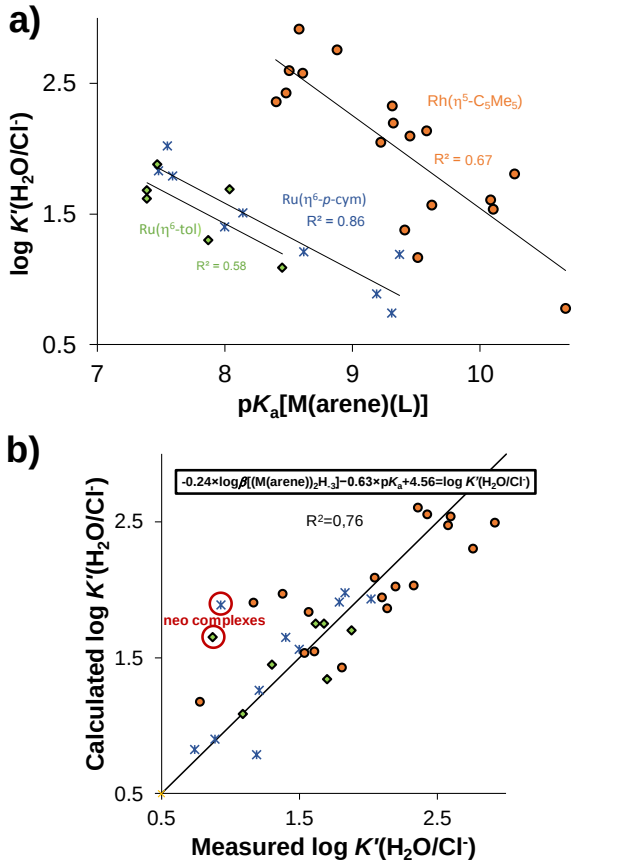

Fig. 8 a) The measured log $K'(H_2O/Cl^-)$ values of [M(arene)(L)] complexes in the function of their pK_a[M(arene)(L)] constants (I = 0.20 M (KNO_3)). b) Multilinear regression for calculating log $K'(H_2O/Cl^-)$ based on the shown equation. Used data are collected in Table S6.[22,29,30,45,46,49,52-56] Outlier points are circled.

constant; all used data are summarized in Table S6). The displayed constants (Figure 8.a) are in three different groups with their own fitting lines. However, applying multilinear regression and the log $\beta[(M(arene))_2H_{-3}]$ constants arranged the values in one group (Figure 8.b). The equation of this regression is:

$$-0.24\times\log\beta[(M(arene))_2H_{-3}] - 0.63\times pK_a[M(arene)(L)] + 4.56 = \log K'(H_2O/Cl^-)$$

The first term of this equation takes the M(arene) part into consideration, while the second term describes the effect of bidentate ligand. This model is universal, as it can predict the chloride ion affinity of different half-sandwich M(arene) complexes, if the log $\beta[(M(arene))_2H_{-3}]$ and pK_a[M(arene)(L)] constants are known. The main drawback is that only chloride ion free pK_a[M(arene)(L)] values are acceptable in this model.

After determining those constants, which govern the speciation in solution, we can compare them and find connections with cytotoxicity. In Figure 9 the basicity corrected stability constant, the

pK_a[M(arene)(L)] values, the chloride ion affinity, the cytotoxicity against MES-SA cell line and resistance ratios in the same cell lines are shown for all complexes.

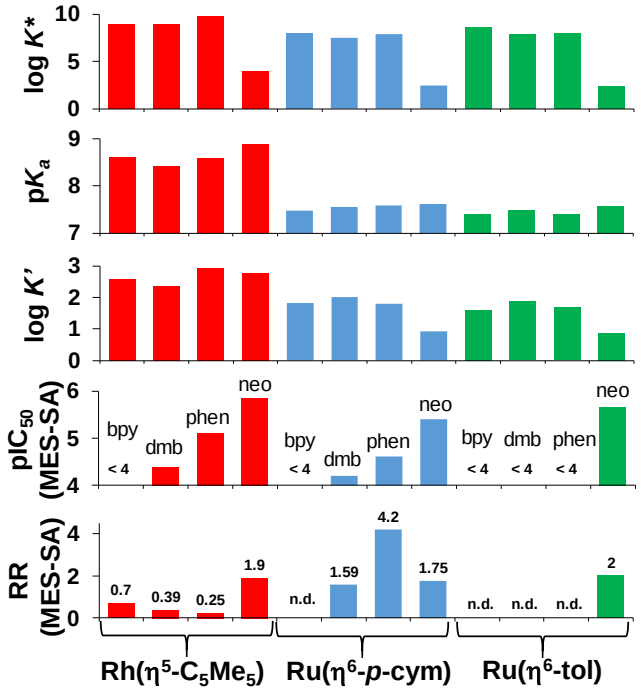

Fig. 9 Comparison of the determined constants: basicity corrected stability constants (log *K**), proton dissociation constants of coordinated water molecules (pK_a), water-chloride exchange constants (log *K*'), the cytotoxicity in MES-SA cell lines (pIC_{50}) and resistance ratio in MES-SA cell lines. N.d.=not determined.

It is clearly seen that methylation of ligand improves anticancer activity. Although neocuproine complexes have the highest cytotoxicity, they have lower stability as compared to the other complexes, suggesting that they might be ligand carriers. High-stability complexes of Ru(η^6-tol) are likely to lose their arene ligands. This process can explain the loss of cytotoxicity and may occur for Ru(η^6-*p*-cym) complexes as well. The MDR-selective complexes show the highest complex stability from all, combined with high pK_a and high chloride ion binding capability. However, the difference between these MDR-selective complexes and the non-selective $[Rh(\eta^5\text{-}C_5Me_5)(bpy)(H_2O)]^{2+}$ complex is not evident because of the slight differences in the respective constants. Together these data suggest that further factors should be considered, such as lipophilicity, redox potential or a specific interaction with a bio-ligand.[44]

Conclusions

Complexes of the half-sandwich $[Ru(\eta^6\text{-}p\text{-cym})(H_2O)_3]^{2+}$, $[Ru(\eta^6\text{-tol})(H_2O)_3]^{2+}$ and $[Rh(\eta^5\text{-}C_5Me_5)(H_2O)_3]^{2+}$ organometallic cations formed with polypiridyl ligands were compared regarding their differences in structural, cytotoxic and aqueous solution behaviour. The structurally related bpy, dmb, phen and neo and their complexes were examined to investigate the effect of methylation and complexation of the ligands. Synthesis of complexes was performed in moderate-to-excellent yields. Based on the X-ray crystallographically determined structures, the change from *p*-cymene to toluene has only a negligible effect on the complex structure, while in the investigated Rh complexes, longer bonds between the bidentate ligands and the metal centre could be found. The methyl groups distorted the structure, when they are present next to the coordinating atoms, namely there is an angle between the plane of the arene and the plane of bidentate ligand. The polypyridines and their complexes show anticancer activity in A2780 and MES-SA cancer cell lines; however, in A2780cis cell lines they have reduced effect. Phen and dmb and their half-sandwich Rh complexes showed paradoxical toxicity against multidrug resistant MES-SA/Dx5 cells. Interestingly, in all cases coordination to Ru caused a loss of activity and selectivity of these ligands.

Generally, metal complexes with the structure $[M(arene)(N,N)(H_2O)]^{2+}$ show high stability, although stability constants could be determined only for Rh complexes by ligand competition studies. In case of neocuproine, the methyl groups next to the nitrogen atoms lower the stability of complexes due to steric congestion with the arene. This is clearly shown, when log *K** (stability constant in which the different basicity of the ligand is taken into account) of complexes are compared with each other: 9.78 (phen) > 9.01 (dmb) > 8.89 (bpy) > 3.93 (neo). The pK_a value of coordinated water molecule is between 7.39-7.62 for Ru and 8.40-8.88 for Rh compounds; thus, methylation has a small effect on this constant. Methyl groups have a great effect on the $K'(H_2O/Cl^-)$ constants of Ru compounds containing neocuproine, decreasing them with one order of magnitude compared to 1,10-phenantroline (log $K'(H_2O/Cl^-)$ = 1.79 *vs.* 0.93 for *p*-cymene and 1.68 *vs.* 0.87 for toluene complexes), which is also in connection with steric hindrance.

A correlation was made between the hydrolytic properties and the water-chloride exchange constants, which is universal for Rh and Ru complexes as well. No direct correlation was seen between the determined equilibrium constants (stability, proton dissociation and chloride/water exchange constants) of these half-sandwich complexes and cytotoxicity. The studied complexes are highly stable, thus the liberation of the bidentate ligands is not likely (except for the neocuproine complexes). The loss of the cytotoxicity of the Ru complexes is suggested to be connected to the slow and irreversible decomposition processes, in which the half-sandwich structure of these Ru(II) complexes is destroyed due to the arene loss, while the bidentate ligand remains coordinated.

Experimental

Chemicals

All solvents were of analytical grade and used without further purification. 1,10-phenanthroline, neocuproine, 2,2'-bipyridine, 4,4'-dimethyl-2,2'-bipyridine, ethylenediamine, $[Rh(\eta^5\text{-}C_5Me_5)(\mu\text{-}Cl)Cl]_2$, $[Ru(\eta^6\text{-}p\text{-cym})(\mu\text{-}Cl)Cl]_2$, $RuCl_3 \times 3\ H_2O$, 1-fmethyl-1,4-cyclohexadiene, doxorubicin, cisplatin, KCl, $AgNO_3$, $Ag(CF_3SO_3)$, HNO_3, KOH, 4,4-dimethyl-4-silapentane-1-sulfonic acid (DSS),

Dulbecco's Modified Eagle Medium (DMEM), RPMI 1640 with FBS, NaH_2PO_4, Na_2HPO_4 and KH_2PO_4 were purchased from Sigma-Aldrich in *puriss* quality. The P-gp inhibitor tariquidar is from Dr. S. Bates (NCI NIH). Ultrapure Milli-Q water was used for sample preparation. [M(arene)(N,N)Cl]Cl complexes were synthesized as previously described.[11,31-33] Synthesis, yields and characterization is described in the Electronic Supplementary Information as well as characterization methods in details (ESI-MS, NMR and single crystal X-ray crystallography[57-62]). $[Ru(\eta^6\text{-tol})(\mu\text{-Cl})Cl]_2$ was prepared according to literature procedures,[63] as well as 5-chloro-7-(1-*L*-prolinylmethyl)-8-hydroxyquinoline.[30]

The exact concentration of the ligand stock solutions together with the proton dissociation constants were determined by pH-potentiometric titrations with the use of the computer program Hyperquad2013,[64], Irving method[65] and the water ionization constant (K_w = 13.76).[66] Detailed description of pH-potentiometry can be found in ESI. The aqueous $[Rh(\eta^5\text{-}C_5Me_5)(H_2O)_3](NO_3)_2$, $[Ru(\eta^6\text{-}p\text{-cym})(H_2O)_3](NO_3)_2$ and $[Ru(\eta^6\text{-tol})(H_2O)_3](NO_3)_2$ stock solutions were obtained by dissolving an exact amount of the dimeric precursor in water followed by addition of equivalent amounts of $AgNO_3$ and filtration of AgCl precipitate. The exact concentrations of chloride-free metal ion stock solutions were determined by pH-potentiometric titrations employing stability constants for $[(Rh(\eta^5\text{-}C_5Me_5))_2(\mu\text{-}OH)_i]^{(4-i)+}$, $[(Ru(\eta^6\text{-tol}))_2(\mu\text{-}OH)_i]^{(4-i)+}$ and $[(Ru(\eta^6\text{-}p\text{-cym}))_2(\mu\text{-}OH)_i]^{(4-i)+}$ (i = 2 or 3) complexes.[45,46] Stock solutions of dmb and neo were prepared with HNO_3 to increase solubility, exact concentrations were calculated from the weight-in-volume basis.

The buffered samples were prepared in 20 mM phosphate buffer or in a modified phosphate buffered saline (PBS') at pH 7.40. PBS' contains 12 mM Na_2HPO_4, 3 mM KH_2PO_4, 1.5 mM KCl and 100.5 mM NaCl; and the concentration of the K^+, Na^+ and Cl^- ions corresponds to that of the human blood serum. Phosphate is the best choice for the pH range 6.0-7.4 because mostly it does not coordinate to these metal ions (except RAED complexes *vide supra*).

UV-Vis spectrophotometric and ^{1}H NMR specroscopy

An Agilent Cary 8454 diode array spectrophotometer was used to record the UV-Vis spectra in the interval 200–800 nm. The path length was 0.5 or 1 cm. Only one of the proton dissociation constants of neo and dmb could be determined by spectrophotometric titrations. Complex formation kinetics was investigated with the use of tandem cuvette. Deprotonation of coordinated water molecule in complexes was followed by spectrophotometry. UV-Vis spectra were used to investigate the H_2O/Cl^- exchange processes of complexes at 200 μM concentration (500 μM for en complexes), around pH 6.0 (20 mM phosphate buffer) as a function of chloride concentrations (0–310 mM).

NMR spectroscopic studies were carried out on a Bruker Avance III HD Ascend 500 Plus instrument. For aqueous samples ^{1}H NMR spectra were recorded with the WATERGATE water suppression pulse scheme using DSS internal standard. Deprotonation of coordinated water molecule in complexes was also followed by ^{1}H NMR. Samples were made in a 10% (v/v) D_2O/H_2O mixture and were titrated at 25.0 °C, at *I* = 0.20 M (KNO_3) at 1:1 metal-to-ligand ratio. The slower kinetic measurements were checked by NMR to see the endpoint of complex formation. Stability constants for the complexes of ethylenediamine and neocuproine were calculated by the computer program PSEQUAD[67] based on ^{1}H NMR spectra.

In vitro cell studies

Cell lines and culture conditions

The human ovarian cancer cell line A2780 and its cisplatin resistant (A2780cis) counterpart, human uterine sarcoma cell lines MES-SA and the doxorubicin selected MES-SA/Dx5 were obtained from ATCC (American Type Culture Collection) (MES-SA: No. CRL-1976™, MES-SA-MES-SA/Dx5: No. CRL-1977™). The phenotype of the resistant cells was verified using cytotoxicity assays (Tables 1, 2 and S5, doxorubicin and cisplatin). Cells were cultivated in Dulbecco's Modified Eagle Medium (DMEM, Sigma-Aldrich) and supplemented with 10% fetal bovine serum, 5 mM glutamine, and 50 units per mL penicillin and streptomycin (Life Technologies). All cell lines were cultivated at 37 °C under a humidified atmosphere containing 95% air and 5% CO_2.

Cell viability assay

Cytotoxic effects were determined by the colorimetric microculture MTT assay.[68] Cells were harvested from culture flasks by trypsinization, seeded in 100 μL aliquots into 96-well microculture plates (Sarstedt, Newton, USA) at 5000 cells per well and allowed to settle and resume exponential growth in drug-free complete culture medium for 12 h to 24 h. Ligands and complexes were diluted in complete culture medium and added to the plates. The complexes of the ligands were prepared in situ by mixing the ligand with an equimolar concentration of the organometallic cations using their stock solutions containing known amounts of $[Rh(\eta^5\text{-}C_5Me_5)(H_2O)_3]^{2+}$, $[Ru(\eta^6\text{-}p\text{-cymene})(H_2O)_3]^{2+}$ and $[Ru(\eta^6\text{-toluene})(H_2O)_3]^{2+}$. Following the addition of the serial dilutions of ligands and complexes and an incubation period of 72 h, the supernatant was removed and fresh medium supplemented with the MTT reagent (0.83 mg/mL) was added. Incubation with MTT at 37 °C was terminated after 1 h by removing the supernatants and lysing the cells with 100 μL DMSO per well. Viability of the cells was measured spectrophotometrically by absorbance at 540 nm using an EnSpire microplate reader. Data were background corrected by subtraction of the signal obtained from unstained cell lysates and normalized to untreated cells. Curves were fitted with the Prism software[69] using the sigmoidal dose–response model (comparing variable and fixed slopes). Curve fit statistics were used to determine the concentration of the test compound that resulted in 50% toxicity (IC_{50}). Evaluation is based on means from three independent experiments, each comprising three replicates per each concentration. Co-incubation experiments were also performed in the presence of the P-gp inhibitor tariquidar. Doxorubicin and cisplatin were used as positive controls.

Conflicts of interest

There are no conflicts to declare.

Acknowledgements

This work was supported by the National Research, Development and Innovation Office-NKFIA through projects GINOP-2.3.2-15-2016-00038, FK 124240, PD 128504, KH129588, 2018-1.2.1-NKP-2018-00005 (financed under the 2018-1.2.1-NKP funding scheme) and Ministry of Human Capacities, Hungary grant, TKP-2020. GS and EAE were supported by a Momentum Grant of the Hungarian Academy of Sciences.

References

1. S. M. Meier-Menches, C. Gerner, W. Berger, C. G. Hartinger and B. K. Keppler, *Chem. Soc. Rev.*, 2018, **47**, 909–928. DOI: 10.1039/C7CS00332C
2. R. E. Aird, J. Cummings, A. A. Titchie, M. Muir, R. E. Morris, H. Chen, P. J. Sadler and D. I. Jodrell, *Br. J. Cancer*, 2002, **86**, 1652–1657. DOI: 10.1038/sj/bjc/6600290
3. A. Habtemariam, M. Melchart, R. Fernández, S. Parsons, I. D. H. Oswald, A. Parkin, F. P. A. Fabbiani, J. E. Davidson, A. Dawson, R. E. Aird, D. I. Jodrell and P. J. Sadler, *J. Med. Chem.*, 2006, **49**, 6858–6868. DOI: 10.1021/jm060596m
4. Z. Adhireksan, G. E. Davey, P. Campomanes, M. Groessl, C. M. Clavel, H. Yu, A. A. Nazarov, C. H. F. Yeo, W. H. Ang, P. Dröge, U. Rothlisberger, P. J. Dyson and C. A. Davey, *Nat. Commun.*, 2014, **5**, No. 3462. DOI: 10.1038/ncomms4462
5. Z. Almodares, S. J. Lucas, B. D. Crossley, A. M. Basri, C. M. Pask, A. J. Hebden, R. M. Phillips and P. C. McGowan, *Inorg. Chem.*, 2014, **53**, 727–736. DOI: 10.1021/ic401529u
6. A. Mitrovic, J. Kljun, I. Sosic, M. Ursic, A. Meden. S. Gobec, J. Kos and I. Turel, *Inorg. Chem.*, **58**, 12334–12347. DOI: 10.1021/acs.inorgchem.9b01882
7. X. Zhang, F. Ponte, E. Borfecchia, A. Martini, C. Sanchez-Cano, E. Sicilia and P. J. Sadler, *Chem. Commun.* 2019, **55**, 14602–14605. DOI: 10.1039/c9cc06725f
8. S. J. Dougan, A. Habtemariam, S. E. McHale, S. Parsons and P. J. Sadler, *PNAS*, 2008, **105**, 11628–11633. DOI: 10.1073/pnas.0800076105
9. J. J. Soldevila-Barreda and P. J. Sadler, *Curr. Opin. Chem. Biol.*, 2015, **25**, 172–183. DOI: 10.1016/j.cbpa.2015.01.024
10. S. Banerjee and P. J. Sadler, *RSC Chem. Biol.*, 2021, **2**, 12–29 DOI: 10.1039/d0cb00150c
11. P. K. Anuja and P. Priyankar, *J. Inorg. Biochem.*, 2020, **208**, No. 111099 DOI: 10.1016/j.jinorgbio.2020.111099
12. J. Valladolid, C. Hortigüela, N. Busto, G. Espino, A. M. Rodríguez, J. M. Leal, F. A. Jalón, B. R. Manzano, A. Carbayo and B. García, *Dalton Trans.*, 2014, **43**, 2629–2645. DOI: 10.1039/c3dt52743c
13. L. Colina-Vegas, W. Villareal, M. Navarro, C. R. de Oliveira, A. E. Graminha, P. I. da S. Maia, V. M. Deflon, A. G. Ferreira, M. R. Cominetti and A. A. Batista, *J. Inorg. Biochem.*, 2015, **153**, 150–161. DOI: 10.1016/j.jinorgbio.2015.07.016
14. Y. Geldmacher, M. Oleszak and W. S. Sheldrick, *Inorg. Chim. Acta*, 2012, **393**, 84–102. DOI: 10.1016/j.ica.2012.06.046
15. D. L. Ma, C. Wu, K. J. Wu and C. H Leung, *Molecules*, 2019, **24**, 2739–2753. DOI: 10.3390/molecules24152739
16. C. C. Konkankit, S. C. Marker, K. M. Knopf and J. J. Wilson, *Dalton Trans.*, 2018, **47**, 9934–9974. DOI: 10.1039/c8dt01858h
17. A. F. A. Peacock, A. Habtemariam, S. A. Moggach, A. Prescimone, S. Parsons and P. J. Sadler, *Inorg. Chem.*, 2007, **46**, 4049–4059. DOI: 10.1021/ic062350d
18. F. E. Poynton, S. A. Bright, S. Blasco, D. C. Williams, J. M. Kelly and T. Gunnlaugsson, *Chem. Soc. Rev.*, 2017, **46**, 7706–7756. DOI: 10.1039/c7cs00680b
19. P. K. L. Fu and C. Turro, *Chem. Commun.*, 2001, 279–280. DOI: 10.1039/b007816f
20. M. A. Scharwitz, I. Ott, Y. Geldmacher, R. Gust and W. S. Sheldrick, *J. Organomet. Chem.*, 2008, **693**, 2299–2309. DOI: 10.1016/j.jorganchem.2008.04.002
21. S. Schäfer, I. Ott, R. Gust and W. S. Sheldrick, *Eur. J. Inorg. Chem.*, 2007, 3034–3046. DOI: 10.1002/ejic.200700206
22. J. P. Mészáros, O. Dömötör, C. M. Hackl, A. Roller, B. K. Keppler, W. Kandioller and É. A. Enyedy, *New J. Chem.*, 2018, **42**, 11174–11184. DOI: 10.1039/C8NJ01681J
23. J. F. Kou, C. Qian, J. Q. Wang, X. Chen, L. L. Wang, H. Chao and L. N. Ji, *J. Biol. Inorg. Chem.*, 2012, **17**, 81–96. DOI: 10.1007/s00775-011-0831-6
24. T. Trobec, M. C. Žužek, K. Sepčić, J. Kladnik, J. Kljun, I. Turel, E. Benoit and R. Frangež, *Biomed. Pharmacother.*, 2020, **127**, 110161. DOI: 10.1016/j.biopha.2020.110161
25. G. Szakács, M. D. Hall, M. M. Gottesman, A. Boumendjel, R. Kachadourian, B. J. Day, H. Baubichon-Cortay and A. Di Pietro, *Chem. Rev.*, 2014, **114**, 5753–5774. DOI: 10.1021/cr4006236
26. M. M. Gottesman, O. Lavi, M. D. Hall and J. P. Gillet, *Annu. Rev. Pharmacol. Toxicol.*, 2016, **56**, 85–102. DOI: 10.1146/annurev-pharmtox-010715-103111
27. H. Zahreddine and K. L. B. Borden, *Front. Pharmacol.* 2013, **4**, No. 28. DOI: 10.3389/fphar.2013.00028
28. L. Côrte-Real, R. G. Teixeira, P. Gírio, E. Comsa, A. Moreno, R. Nasr, H. Baubichon-Cortay, F. Avecilla, F. Marques, M. P. Robalo, P. Mendes, J. P. P. Ramalho, M. H. Garcia, P. Falson and A. Valente, *Inorg. Chem.*, 2018, **57**, 4629–4639. DOI: 10.1021/acs.inorgchem.8b00358
29. O. Dömötör, V. F. S. Pape, N. V. May, G. Szakács and É. A. Enyedy, *Dalton Trans.*, 2017, **46**, 4382–4396. DOI: 10.1039/c7dt00439g
30. J. P. Mészáros, J. M. Poljarević, I. Szatmári, O. Csuvik, F. Fülöp, N. Szoboszlai, G. Spengler and É. A. Enyedy, *Dalton Trans.*, 2020, **49**, 7977–7992. DOI: 10.1039/D0DT01256D
31. T. K. Todorova, T. N. Huan, X. Wang, H. Agarwala and M. Fontecave, *Inorg. Chem.*, **58**, 6893–6903. DOI: 10.1021/acs.inorgchem.9b00371
32. J. M. de Ruiter, R. L. Purchase, A. Monti, C. J. M. van der Ham, M. P. Gullo, K. S. Joya, M. D'Angelantonio, A. Barbieri, D. G. H. Hetterscheid, H. J. M. de Groot and F. Buda, *ACS Catal.*, 2016, **6**, 7340–7349. DOI: 10.1021/acscatal.6b02345
33. J. Canivet and G. Süss-Fink, *Green Chem.*, 2007, **9**, 391–397. DOI: 10.1039/b612518b
34. S. J. Dougan, M. Melchart, A. Habtemariam, S. Parsons and P. J. Sadler, *Inorg. Chem.*, 2006, **45**, 10882–10894. DOI: 10.1021/ic061460h
35. F. Wang, H. Chen, S. Parsons, I. D. H. Oswald, J. E. Davidson and P. J. Sadler, *Chem. Eur. J.*, 2003, **9**, 5810–5820. DOI: 10.1002/chem.200304724

36. S. Ogo, H. Hayashi, K. Uehara and S. Fukuzumi, *Appl. Organometal. Chem.*, 2005, **19**, 639−643. DOI: 10.1002/aoc.837
37. M. C. Carrión, M. Ruiz-Castañeda, G. Espino, C. Aliende, L. Santos, A. M. Rodríguez, B. R. Manzano, F. A. Jalón and A. Lledós, *ACS Catal.*, 2014, **4**, 1040−1053.
38. O. V. Dolomanov, L. J. Bourhis, R. J. Gildea, J. A. K. Howard and H. Puschmann, *J. Appl. Cryst.*, 2009, **42**, 339−341. DOI: 10.1107/S0021889808042726
39. I. A. Guzei and M. Wendt, *Dalton Trans.*, 2006, 3991−3999. DOI: 10.1039/B605102B
40. D. Türk, M. D. Hall, B. F. Chu, J. A. Ludwig, H. M. Fales, M. M. Gottesman and G. Szakács, *Cancer Res.*, 2009, **69**, 8293−8301. DOI: 10.1158/0008-5472.CAN-09-2422
41. A. Füredi, Sz. Tóth, K. Szebényi, V. F. S. Pape, D. Türk, N. Kucsma, L. Cervenak, J. Tóvári, G. Szakács, *Mol. Cancer Ther.*, 2017, **16**, 45−56. DOI: 10.1158/1535-7163.MCT-16-0333-T
42. S. Betanzos-Lara, O. Novakova, R. J. Deeth, A. M. Pizarro, G. J. Clarkson, B. Liskova, V. Brabec, P. J. Sadler and A. Habtemariam, *J. Biol. Inorg. Chem.*, 2012, **17**, 1033−1051. DOI: 10.1007/s00775-012-0917-9
43. G. Chao, W. Hong-Yan, D. Yi-Li, L. Ji, X. Yun, G. Qiu-Yu, S. Zhi, Q. Yong, P. J. Sadler and L. Hong-Ke, *Chinese J. Inorg. Chem.*, 2018, **34**, 1079−1085. DOI: 10.11862/CJIC.2018.148
44. M. Cserepes, D. Türk, Sz. Tóth, V. F. S. Pape, A. Gaál, M. Gera, J. E. Szabó, N. Kucsma, Gy. Várady, B. G. Vértessy, C. Streli, P. T. Szabó, J. Tovari, N. Szoboszlai and G. Szakács, *Cancer Res.*, 2020, **80**, 663–674. DOI: 10.1158/0008-5472.CAN-19-1407
45. O. Dömötör, S. Aicher, M. Schmidlehner, M. S. Novak, A. Roller, M. A. Jakupec, W. Kandioller, C. G. Hartinger, B. K. Keppler and É. A. Enyedy, *J. Inorg. Biochem.*, 2014, **134**, 57−65. DOI: 10.1016/j.jinorgbio.2014.01.020
46. L. Bíró, A. J. Godó, Z. Bihari, E. Garribba and P. Buglyó, *Eur. J. Inorg. Chem.*, 2013, **2013**, 3090−3100. DOI: 10.1002/ejic.201201527
47. H. A. Schwartz, C. Creutz and N. Sutin, *Inorg. Chem.*, 1985, **24**, 433−439. DOI: 10.1021/ic00197a036
48. G. D. Stevens and R. A. Holwerda, *Inorg. Chem.*, 1984, **23**, 2777−2780. DOI: 10.1021/ic00186a013
49. É. A. Enyedy, J. P. Mészáros, O. Dömötör, C. M. Hackl, A. Roller, B. K. Keppler, W. Kandioller, *J. Inorg. Biochem.*, 2015, **152**, 93−103. DOI: 10.1016/j.jinorgbio.2015.08.025
50. H. Chen, J. A. Parkinson, R. E. Morris and P. J. Sadler, *J. Am. Chem. Soc.*, 2003, **125**, 173−186. DOI: 10.1021/ja027719m
51. A. M. Pizarro, A. Habtemariam and P. J. Sadler, *Top. Organomet. Chem.*, 2010, **32**, 21−56. DOI: 10.1007/978-3-642-13185-1_2
52. O. Dömötör, C. M. Hackl, K. Bali, A. Roller, M. Hejl, M. A. Jakupec, B. K. Keppler, W. Kandioller and É. A. Enyedy, *J. Organomet. Chem.*, 2017, **846**, 287−295. DOI: 10.1016/j.jorganchem.2017.06.027
53. É. A. Enyedy, O. Dömötör, C. M. Hackl, A. Roller, M. S. Novak, M. A. Jakupec, B. K. Keppler and W. Kandioller, *J. Coord. Chem.*, 2015, **68**, 1583−1601. DOI: 10.1080/00958972.2015.1023195
54. É. Sija, C. G. Hartinger, B. K. Keppler, T. Kiss and É. A. Enyedy, *Polyhedron*, 2014, **67**, 51−58. DOI: 10.1016/j.poly.2013.08.057
55. É. A. Enyedy, É. Sija, T. Jakusch, C. G. Hartinger, W. Kandioller, B. K. Keppler and T. Kiss, *J. Inorg. Biochem.*, 2013, **127**, 161−168.
56. J. M. Poljarević, G. T. Gál, N. V. May, G. Spengler, O. Dömötör, A. R. Savić, S. Grgurić-Šipka and É. A. Enyedy, *J. Inorg. Biochem.*, 2018, **181**, 74−85. DOI: 10.1016/j.jinorgbio.2017.12.017
57. T.Higashi, *Numerical Absorption Correction*, NUMABS, 2002
58. *CrystalClear SM 1.4.0*, Rigaku/MSC Inc., 2008
59. *SHELXL-2013 Program for Crystal Structure Solution*, University of Göttingen, Germany, 2013
60. L. J. Farrugia, *J. Appl. Crystallogr.*, 2012, **45**, 849−854. DOI: 10.1107/S0021889812029111
61. A. L. Spek, *J. Appl. Crystallogr.*, 2003, **36**, 7−13. DOI: 10.1107/S0021889802022112
62. S. P. Westrip, *J. Appl. Crystallogr.*, 2010, **43**, 920−925. DOI: 10.1107/S0021889810022120
63. R. A. Zelonka and M. C. Baird, *Can. J. Chem.*, 1972, **50**, 3063−3072. DOI: 10.1139/v72-486
64. P. Gans, A. Sabatini and A. Vacca, *Talanta*, 1996, **43**, 1739–1753. DOI: 10.1016/0039-9140(96)01958-3
65. H. M. Irving, M. G. Miles and L. D. Petit, *Anal. Chim. Acta*, 1967, **38**, 475–482. DOI: 10.1016/S0003-2670(01)80616-4
66. *SCQuery, The IUPAC Stability Constants Database*, Academic Software (Version 5.5), R. Soc. Chem., 1993–2005.
67. L. Zékány and I. Nagypál in *Computational Methods for the Determination of Stability Constants*, ed. D. L. Leggett, Plenum Press, New York, 1985, pp. 291–353.
68. K. Juvale, V. F. S. Pape and M. Wiese, *Bioorg. Med. Chem.*, 2012, **20**, 346–355. DOI: 10.1016/j.bmc.2011.10.074
69. *GraphPad Prism version 8.0.0 for Windows*, GraphPad Software, La Jolla, California USA, 2020 http://www.graphpad.com (accessed 12.11.2020)